Remote Sensing of Land
Homepage: www.gathacognition.com/journal/gcj1
http://dx.doi.org/10.21523/gcj1

Original Research Paper

Improved Change Detection of Forests Using Landsat TM and ETM+ data

Kishor R. Sonawane* and Vijay S. Bhagat

Post-graduate Research Centre in Geography, Agasti Arts, Commerce and Dadasaheb Rupwate Science College, Akole-422601, Ahmednagar, Maharashtra (India).

Abstract

Landsat TM and ETM+ datasets are useful for forest change detection (FCD) at good accuracy level. Classified forest maps have been prepared using NDVI calculated from Landsat-5 TM (2009) and Landsat-7 ETM+ (2002) datasets for FCD using post-classification technique. About 58.59% of reviewed area shows positive changes, 33.69% no-changes and 7.72% negative changes with 77.84% accuracy. This accuracy insists limitations of present FCD analysis. Therefore, improved post-classification technique was formulated for precise FCD using field data and statistical techniques. Information about stable land surface (water bodies, rocky lands, deep forests, etc.) was used for normalization of exaggerated reflectance in vegetation indices i.e. greenness. About 70.08% land estimated using second approach shows stable vegetation, 23.59% positive changes and 6.33% negative changes. Higher accuracy (95.21%) itself shows improvement in FCD technique and efficient applicability for sustainable land management.

Article history

Received: 15 November 2016
In revised form: 10 February 2017
Accepted: 12 February 2017

Keywords

Landsat-5 TM,
Landsat-7 ETM+,
NDVI,
LST,
Tasseled Cap Coefficient,
Forest Change Detection.

Editor(s)

V.S. Bhagat

1 INTRODUCTION

A forest is a community of living organisms which interact mutually with the physical environment. Forest covers approximately 30% (Carlowicz, 2012) to 31% (FAO, 2015) of the earth surface with complexities and self-regenerating capacities (Bauer et al., 1994; Virk and King, 2006; Healey *et al.*, 2008). It is a source of organic carbon, which helps to maintain planetary climate, freshwater, biodiversity and useful to manage hazards like soil erosion, landslides, floods, etc. They are habitat of wildlife and regulate different cycles including hydrological, nutrient, atmospheric, etc. and conserve soils, water, etc. (Southworth, 2004).

Land under natural forest is estimated about 33.36 million km² (World Resources Institute [WRI]) to 39.88 million km² (World Conservation Monitoring Centre [WCMC]) excluding marine forests (Mishra *et al.*, 2003; Kumsap *et al.*, 2005; Fettig *et al.*, 2007; Forkuo and Frimpong, 2012). However, from last some decades forest destruction and land appropriation increase, globally (Turker and Derenyi, 2000). Land under forest in India declined to 21.31% of Total Geographical Area (TGA) (ISFR, 2009 and FSI 2015) due to imbalance climatic conditions, soil degradation, deforestation, desertification and water stresses in drought conditions. India endowed with an immense variety of forest resources (Southworth, 2004). However, adverse changes in ecosystem are taking place with continuous pressures of an exploding population and the subsequent domestic needs including food, fuel, fodder, timber as well as industrial demands (Keenan *et al.*, 1999). There are significant losses of forests at an alarming rate (Pant *et al.*, 2000; Hayes and Sader, 2001). The 'hotspots' are identified and declared for tropical biodiversity in Western Ghats. These regions are house of rich biodiversity and globally endemic species (Fang and Xu, 2000). However, it is widely believed that the natural vegetation in this tropical region is losing the biodiversity at unprecedented rates (Panigrahy *et al.*, 2010). Around, 275 million rural people (27%) in India are depends on forests for their subsistence and livelihoods (Kim *et al.*, 2011), earning from trade of fuel wood, fodder, bamboo and minor forest products. It is notable that 17% of rural population in India depends on forests to meet their domestic energy (Drescher and Perera, 2010).

* Author address for correspondence
Post-graduate Research Centre in Geography, Agasti Arts, Commerce and Dadasaheb Rupwate Science College, Akole -422601, Ahmednagar, Maharashtra (India). Tel.: +91 8796146048,
Emails: sonawanek86@gmail.com (*K. Sonawane*-Corresponding author); kalpvij@gmail.com (*V. Bhagat*)

http://dx.doi.org/10.21523/gcj1.17010102

Governmental and non-governmental agencies are involved in conservation of forests from last some decades (Cohen *et al.*, 1998). Planning and management for conservation of forest demands reliable information, investigation and analyses (Cohen *et al.*, 1998; Hansen *et al.*, 2000, Hayes and Sader, 2001; Bhagat, 2009). Many analysts have reported sophisticated techniques like remote sensing (Kennedy *et al.*, 2009), geographic information system (Healey *et al.*, 2008), global positioning system along with mathematical and statistical methods (Fettig *et al.*, 2007) for change detection. Estimations of forests cover using satellite data can give satisfactorily results (Cano *et al.*, 2006). Furthermore, change detection analysis can provide analytical data about forest degradation and conservation (Pouliot *et al.*, 2002). However, reliable change detection techniques for forests using remote sensing data remains a challenging task (Coppin *et al.*, 2004; Im *et al.*,2008; Schwilch *et al.*, 2011; Sommer *et al.*, 2011; Bhagat, 2012). The results are susceptible to data quality, technical efficiency and suitability of selected techniques (Bhagat, 2012). Therefore, modified change detection technique designed for this study based on field checks and statistical analyses to get more precise analysis about forest changes (Southworth, 2004). The Landsat-5 TM and Landsat-7 ETM+ datasets have been used for detection of changes in forest cover in the study area. Two approaches have been adopted for this analysis: Approach I) post-classification technique and Approach II) improved post-classification technique (Chandio and Matori, 2011). Changes in forest were detected using post-classification techniques using NDVI (Fettig *et al.*, 2007) calculated for Landsat-5 TM and Landsat-7 ETM+ datasets, whereas normalized indices and coefficients were used for improved approach of change detection.

Change detection analysis provides a thematic views to understand the natural and artificial behavior of changes in land (Sommer *et al.*, 2011) including 1) increase and decrease in area, 2) seasonal changes in forests, snow cover, coastline, ocean water, 3) mapping of floods, landslides, volcanic eruptions, corral rifts, wild animals, birds, 4) changes in near surface atmospheric conditions like temperature, snowfall, rainfall, clouds, fog, storms, and 5) human activities like military actions, observation, planning and management for war areas, coal mining, etc. (Lunetta *et al.*, 2006). Scientists have used different methods of Digital Change Detection (DCD) including classification of multiband satellite data based on image ratio, tasseled cap coefficient, spectral vegetation indices, principal component analysis, change vector methods, threshold based classification, post-classification comparison, univariate image differencing, simultaneous analysis of multi temporal data, fusion approach, spectral classification, algebraic methods, regressions, etc. (Petit and Lambin, 2001; Bhagat, 2012). However, all methods are not ideally suitable, reliable and applicable to all surface change conditions (Du *et al.*, 2002; Bhagat, 2012). Therefore, corrective measure has been suggested to achieve more precise results of forest change detection in this study. Correlation techniques have been used to find the suitable parameter for corrections from different multiband ratios (Coppin and Bauer, 1996) and spectral indices (Huete *et al.*, 2002). Here, correlation and regression (Mountrakis *et al.*, 2010) techniques have been used to determine variables for detection, estimations of exaggerations and corrections using information collected for stable land surface (water bodies, rocky lands, deep forest, etc.). The suggested technique for forest change detection can be useful for land management and especially forests.

2 STUDY AREA

The study area (13859 ha) is a mountainous range between Pravara and Mula river basin from Western (Ghatghar) to Eastern borders (Washere) of Akole tahsil in Ahmednagar District (India) (Figure 1). The altitude varies from 560 to 1646 m Mean Sea Level (MSL). Geologically, this area is formed by basaltic rock (Gareeau *et al.*, 2009) which prevents water to percolate. The depth and water-holding capacity of soils in the region (Zolekar and Bhagat, 2015) varies according to variations in slopes. The soils are very shallow at hilltop and depth increasing to foothill zones (Kumsap *et al.*, 2005). Very shallow loamy, shallow clayey soils are found on the moderate (1°- 3°) and stiff (3°- 6°) slopes. Soil moisture impacts on the distribution of vegetation cover (Mishra *et al.*, 2003). The forest cover varies with height, slopes, soil qualities, rainfall, etc. Foothill zones in Western parts show dense forest than hilltops with thin soils. Annual rainfall varies from 4937 mm at West and 1904 mm at East (Zolekar and Bhagat, 2015). The mean annual maximum and minimum temperatures are 39.80°C and 8.70°C, respectively. Indigenous people are engaged in agricultural activities (Theiler and Perkins, 2011) on land reclaimed from forests and dependent on forests for domestic needs.

3 DATASET AND SOFTWARE

The analyses are based on remotely sensed data (Shalaby *et al.*, 2006), statistical models (Golmehr, 2008) and field check information. The satellite data of Landsat-7 ETM+ (06th Nov. 2002) and Landsat-5 TM (1st Nov. 2009) (accessed on 01 January 2012) has been used for detection of changes in forest cover. Field check data was collected for verification of inferences. The remotely sensed dataset and data obtained in field checks were compiled, merged and loaded in the GIS image processing software, ILWIS v3.4 Academic, ERDAS Imagine v9.2 (© Hexagon) and ArcGIS v9.3 (© ESRI Ltd.). Garmin's Global Positioning System (GPS) was used for ground verification. Correlation analyses was performed using 'Karl Pearson techniques' (Chen *et al.*, 2001; Yang *et al.*, 2014) available in Statistical Packages for the Social Sciences (SPSS © IBM) (Zhang *et al.*, 2002; Fastring and Griffith, 2009).

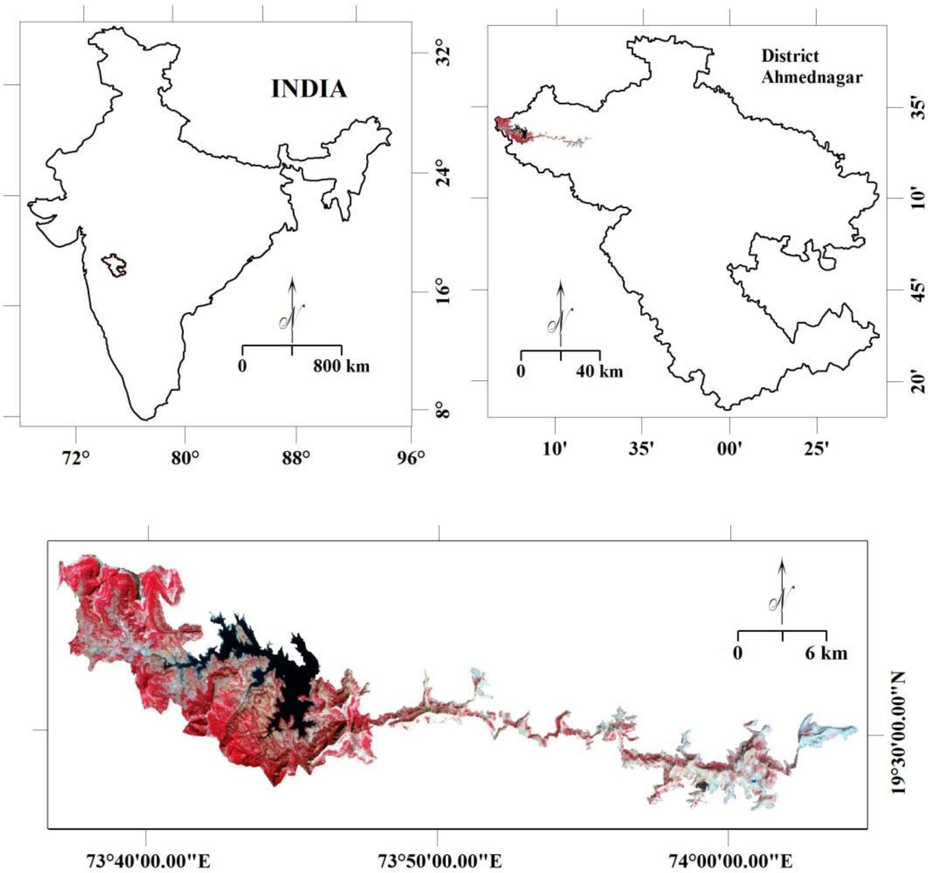

Figure 1. Study area: location map

4 METHODOLOGY AND APPROACHES

Two approaches were used for detection of changes in forest cover: Approach I - post classification technique and Approach II - improved post-classification technique. Accuracy assessment was performed and results of analyses compared to check the applicability of the approaches. Statistical techniques were useful to inculcate robustness in the analysis for change detection (Theiler and Perkins, 2011).

4.1 Co-registration

Matching of multiple images captured at different time is critical task for change detection studies. Mis-registration of images drops accuracy in results obtained in change detection analysis (Burnicki *et al.,* 2010; Bhagat, 2012; Pajares *et al.*, 2012). Authors such as Giri Babu *et al.,* (2014) and Tsai and Lin (2007) have suggested automatic tie point registration, pixel to pixel matching, ground control point registration, semi-automotive registration, etc. to obtained reliable results (Clifton 2003; Julien *et al.,* 2011). Therefore, Landsat-7 ETM+ (t_1) (2002) and Landsat-5 TM (t_2) (2009) scenes were co-registered with the help of: 1) ground truth information (Hara *et al.,* 2012) collected using Garmin GPS device and 2) topo-maps (Survey of India) with pixel to pixel match with 0.00012 Root Mean Square Error (RMSE) in ERDAS Imagine software.

4.2 Image Enhancement

Scientific understanding of behavior and functioning of vegetation landscape, using remotely sensed data with different spectral, radiometric, temporal and spatial resolutions, have been important task in last some decades (Lippitt *et al.,* 2011; Schwilch *et al.,* 2011). Enhancement of images selected for analysis is highly required before further applications like classifications, estimations, etc. (Chowdhury *et al.*, 2005; Weng *et al.,* 2009; Ehlers *et al.,* 2010). Vegetation indices like NDVI, LAI, TVI, etc. (Silleos *et al.*, 2006) have been calculated using different bands e.g. red, infrared, thermal infrared, middle infrared and widely used for detection of land objects. Furthermore, coefficients like Soil Wetness Index (SWI), Normalized Difference Salinity Index (NDSI), Brightness, etc. have been used to study the distribution of soil moisture, soil salinity, etc. Spectral indices viz. NDVI, LAI and Land Surface Temperature Index (LSTI) and Tasseled Cap Coefficient Transformation have been calculated for enhancement of satellite images in present study.

4.2.1 Spectral Indices

In present study, Difference Vegetation Index (DVI), Ratio Vegetation Index (RVI), NDVI, Soil Adjusted Vegetation Index (SAVI), Leaf Area Index **(**LAI), Ratio Difference Vegetation Index (RDVI), Modified SAVI (MSAVI), Infrared Percentage Vegetation Index (IPVI) and Modified Simple Ratio (MSR) (Mróz and Sobieraj, 2004) have been used for change detection analysis. However, NDVI has been widely used for detection of changes in forest cover (Bhagat, 2012). Therefore, NDVI (equation 1) has been calculated using Near Infrared (Band 4) and Red (Band 3) bands of Landsat-7 ETM+ and Landsat-5 TM sensors (Bhagat and Sonawane, 2010).

$$\mathrm{NDVI} = \frac{(\mathrm{NIR-RED})}{(\mathrm{NIR+RED})} \quad (1)$$

Calculated NDVI values vary between -1 to +1 depending on relative Digital Number (DN) of Near Infrared and Red bands. Maximum NDVI (Figure 2) indicates dense vegetation and minimum values represent less or absence of vegetation.

Leaf Area Index (LAI) [m^2/m^2] represents the amount of leaf material in an ecosystem and is geometrically defined as the total one-sided area of photosynthetic tissue per unit ground surface area (Breda, 2003; Jonckheere *et al.*, 2004; Morisette *et al.*, 2006**)**. It appears as a key variable in many models describing vegetation-atmosphere interactions, particularly with respect to the carbon and water cycles (GCOS, 2010). LAI was calculated using following equation after Jensen (2002) (equation 2):

$$LAI = -2.42 + 12.18 * (NDVI) \quad (2)$$

Where, -2.42 and 12.18 are the constants (Jensen, 2002). LAI is widely used to identify and delineate light interception, gross productivity, soil moisture and transpiration from vegetation (Chen *et al.*, 2012). Therefore, LAI were calculated for statistical analysis to test applicability for Forest Change Detection (FCD) in second approach. Furthermore, many scholars have been used Land Surface Temperature Index (LSTI) for vegetation analysis (Yuan and Bauer, 2007). LSTI is measurements of earth surface temperature including canopy, soils, barren lands, rocks, water bodies, snow, ice, roof of a building using satellite data. The DN recorded for satellite images (Julien *et al.*, 2011) were converted (equation 3) using space reaching radiance i.e. Top of Atmosphere (ToA) Radiance (equation 4) (Chander and Markham, 2003).

$$\mathrm{LST(T)} = \frac{k_2}{\mathrm{In}\left(\frac{k_1}{L_\lambda}+1\right)} \quad (3)$$

Here, T is an effective at-satellite temperature in k (kelvin), L_λ is a spectral radiance in W/(m^2 in μm), k_1 and k_2 are pre-launch calibration constants for ETM+ and TM sensors (refer Landsat 7 Science Data Users Handbook by NASA).

$$L_\lambda = \left(\frac{L_{max}-L_{min}}{QCAL_{max}-QCAL_{min}}\right)(DN - QCAL_{min}) + L_{min} \quad (4)$$

Where, L_{max} is a maximum spectral radiance (W/m^2 in μm) at *QCAL* equal 0 DN, L_{min} is a minimum spectral radiance (W/m^2 in μm) at *QCAL* equal 255 DN and $QCAL$ are the quantized calibrated pixel values in DN.

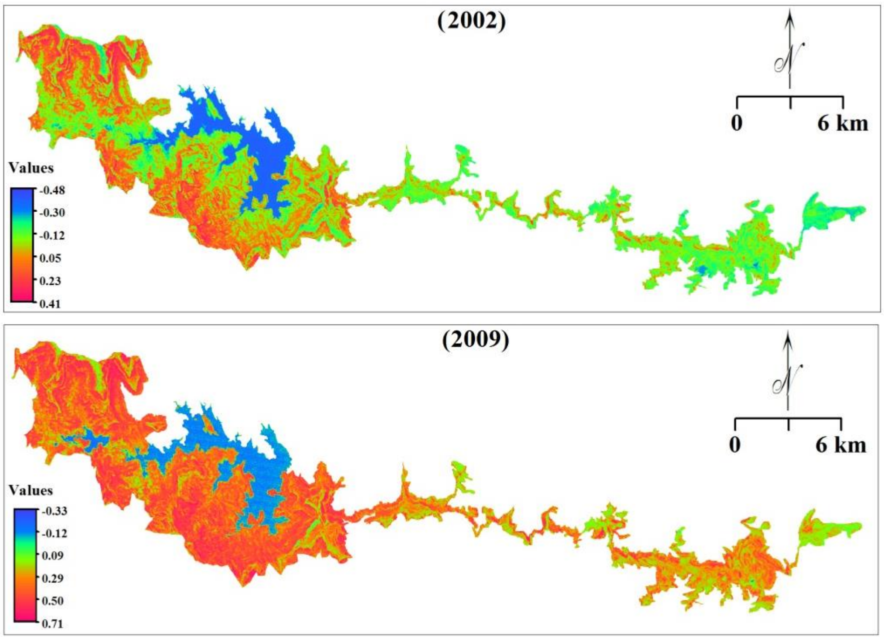

Figure 2. Normalized Difference Vegetation Index (NDVI)

4.2.2 Tasseled Cap Coefficient Transformations (TCCTs)

TCCTs have potentials to derive forest attributes for different regional applications where, atmospheric noise correction not possible (Silleos *et al.*, 2006; Ghosh *et al.*, 2010). These transformations simply reduce the number of radiance noise density and provide high association in single response. Therefore, brightness, greenness, wetness, fourth, fifth and sixth indices were calculated using coefficients estimated by Crist *et al.*, (1986) for Landsat-5 TM (Table 1) and Huang *et al.*, (2002) (Table 2) for Landsat-7 ETM+.

4.3 Approaches of Forest Change Detection

4.3.1 Approach I: Post-classification technique

Satellite images selected for present study was processed for co-registration, enhancements, classification and finally, classified images were compared for Change Detection (CD) in forest cover. Calculated pixel values of NDVI have been broadly grouped into five classes (Table 3) i.e. no-vegetation, low to medium, medium, medium to dense and dense to very dense, using threshold observed in NDVI (2002) and NDVI (2009) images using 'slicing' operation in Ilwis.

The maximum value (0.41) in reference image (t_1) (NDVI 2002) was observed for dense vegetation (Table 3) whereas minimum (-0.48) for barren land including water body, rocky and barren land with 0.05 mean and 0.16 standard deviation. Targeted image (t_2) (NDVI 2009) shows the maximum value (0.71) for dense vegetation and minimum (-0.33) for no-vegetation with 0.31 mean and 0.16 standard deviation. Adegoke and Carleton (2002) have been used innovative hybrid image classification technique for change detection analysis of forest. Therefore, limit values of NDVI classes are different for images acquired for 2002 and 2009 (Table 3) and was decided based on repetitive field checks using GPS, comparison with high-resolution images of Google Earth Pro and FCC (Figure 4). Class 'no-vegetation' includes rocky and barren lands distributed at higher levels (> 1100 m) of mountain and water bodies at bottom (Figure 3).

Table 1. Landsat-5 TM: tasselled cap coefficients at satellite reflectance

Index	Band1	Band2	Band3	Band4	Band5	Band7
Brightness	0.2909	0.2493	0.4806	0.5568	0.4438	0.1706
Greenness	-0.2728	-0.2174	-0.5508	0.7221	0.0733	-0.1648
Wetness	0.1446	0.1761	0.3322	0.3396	-0.6210	-0.4186
Fourth	0.8461	-0.0731	-0.4640	-0.0032	-0.0492	0.0119
Fifth	0.0549	-0.0232	0.0339	-0.1937	0.4162	-0.7823
Sixth	0.1186	-0.8069	0.4094	0.0571	-0.0228	0.0220

Source: Crist *et al.*, 1986

Table 2. Landsat-7 ETM+: tasselled cap coefficients at satellite reflectance

Index	Band1	Band2	Band3	Band4	Band5	Band7
Brightness	0.3561	0.3972	0.3904	0.6966	0.2286	0.1596
Greenness	-0.3344	-0.3544	-0.4556	0.6966	-0.0242	-0.2630
Wetness	0.2626	0.2141	0.0926	0.0656	-0.7629	-0.5388
Fourth	0.0805	-0.0498	0.1950	-0.1327	0.5752	-0.7775
Fifth	-7252	-0.0202	0.6683	0.0631	-0.1494	-0.0274
Sixth	0.4000	-0.8172	0.3832	0.0602	-0.1095	0.0985

Source: Huang *et al.*, 2002

Table 3. Broad classification of forest density based on NDVI

Classes	Index values	
	ETM+ (2002)	TM (2009)
No-vegetation	< -0.16	< 0.20
Low to medium	-0.16 to -0.02	0.20 to 0.23
Medium	-0.02 to 0.01	0.23 to 0.36
Medium to dense	0.01 to 0.16	0.36 to 0.45
Dense to very dense	0.16 <	0.45 <

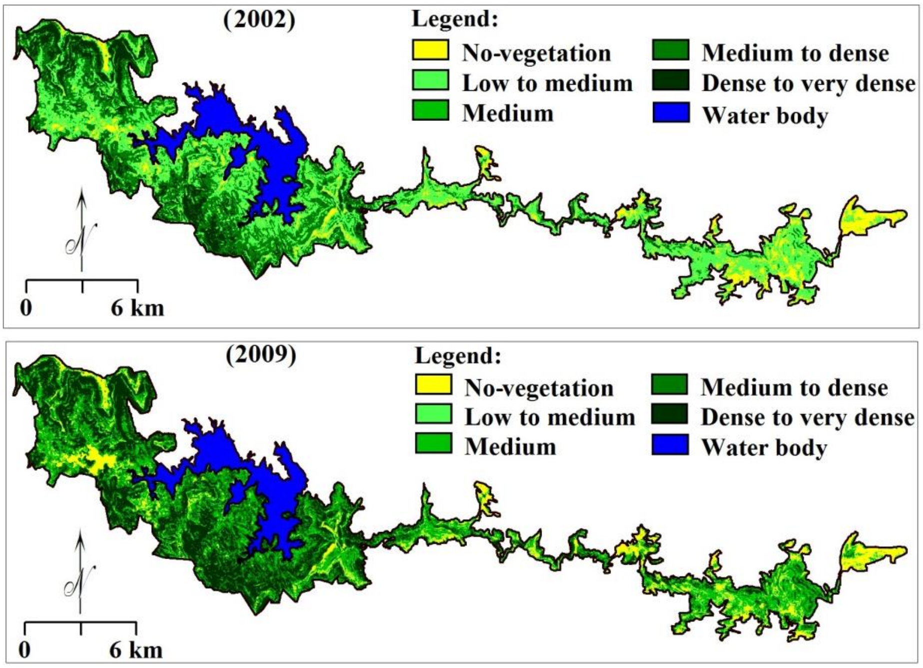

Figure 3. Distribution of forest depicted based on NDVI

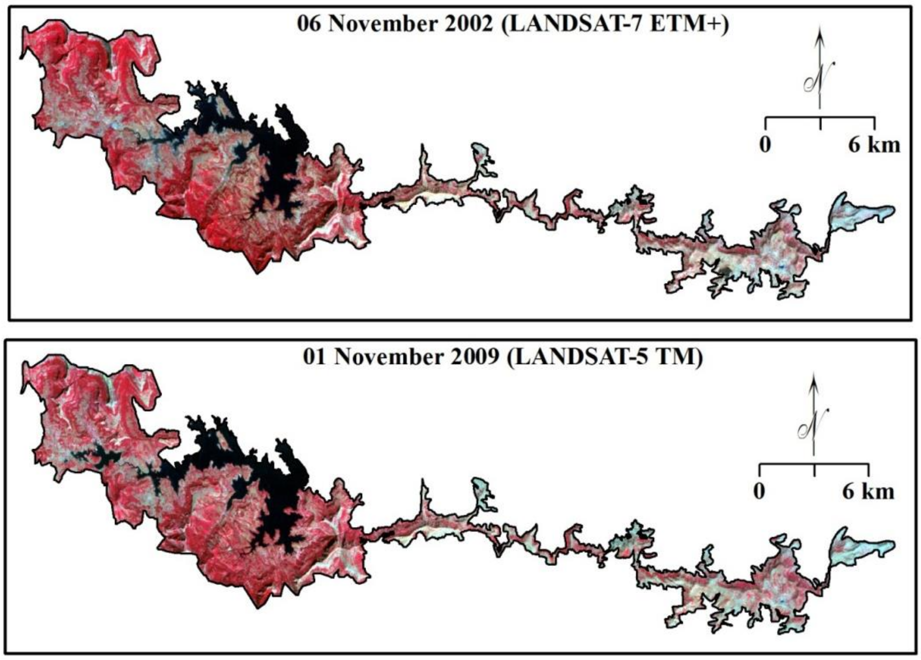

Figure 4. False Color Composite (FCC) images

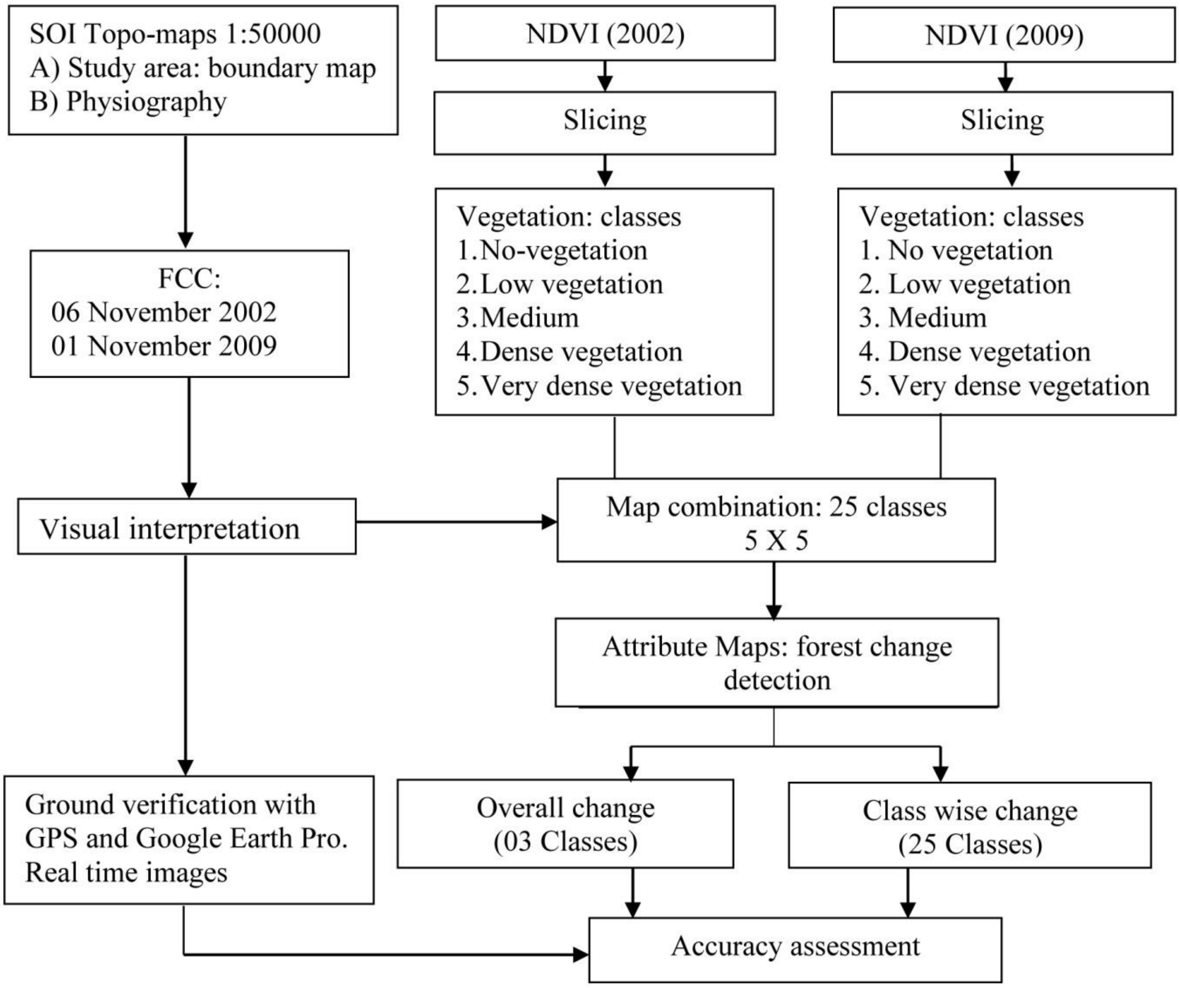

Figure 5. Approach-I: schematic preparation

Measurements of differences between detected land classes in base image (t_1) and target image (t_2) based on radiance difference called change detection (Weng *et al.*, 2009), for instance forest. The radiance difference mainly occurred due to real change in surface features, deviation in atmospheric conditions, deviation in sensor calibration, minimum to maximum error in Route Mean Square (RMS) at the time of georeferencing, deviation in illumination and difference in soil moisture conditions, etc. Here, classified images t_1 and t_2 combined using 'cross' operator (Figure 5) in Ilwis which produce 25 classes (5 classes t_1 X 5 classes t_2). Similar classes have been merged into three classes viz. no-change, positive change and negative change in forest cover (Table 4) using tool 'merging the classes' in Ilwis. Further, class wise changes (Table 11) in forest cover also detected successfully (Figure 14) using same technique (Table 4). However, overall accuracy of the classes detected to show changes in forest cover was estimated about 78%. Users' accuracy for class 'positive change' was about 58% and producer's accuracy 70%. Rozenstein and Karnieli (2011) have insisted vigorous and creative efforts to establish new algorithms for change detection. Therefore, statistical methods and corrective measures were adopted to achieve improvements in post-classification technique for CD in forest cover.

4.3.2 Approach II: Improved post-classification technique

Many scholars have been successfully used combinations of different approaches for CD of land objects (Cano *et al.*, 2006; Pu *et al.*, 2008; Weng *et al.*, 2009). The algorithm of FCD has been modified to improve (Figure 6) the results and processed through five steps: 1) sampling (Chapelle *et al.*, 2002; Lu *et al.*, 2011), 2) statistical analysis (Singh, 1989; Dhakal *et al.*, 2002), 3) normalization of indices, 4) change detection and 5) accuracy assessment. Statistical analysis and information about stable land surface including deep forests, rocky lands, barren lands and water bodies have used for normalization of indices calculated for target image (t_2) (Felkar *et al.*, 1981; Singh, 1996; Turker and Derenyi, 2000).

Table 4. Class merging scheme for overall FCD

Vegetation classes: ETM+ (2002)	Vegetation classes: TM (2009)				
	No-vegetation	**Low to medium**	**Medium**	**Medium to dense**	**Dense to very dense**
No-vegetation	No-change	Positive change	Positive change	Positive change	Positive change
Low to medium	Negative change	No-change	Positive change	Positive change	Positive change
Medium	Negative change	Negative change	No-change	Positive change	Positive change
Medium to dense	Negative change	Negative change	Negative change	No-change	Positive change
Dense to very dense	Negative change	Negative change	Negative change	Negative change	No-change

Table 5. Class merging scheme for class wise FCD

Vegetation classes: ETM+ (2002)	Vegetation classes: TM (2009)				
	No-vegetation	**Low to medium**	**Medium**	**Medium to dense**	**Dense to very dense**
No-vegetation	NVNoC	NVPL	NVPM	NVPD	NVPVD
Low to medium	LNNV	LNoC	LPM	LPD	LPVD
Medium	MNNV	MNL	MNoC	MPD	MPVD
Medium to dense	DNNV	DNL	DNM	DNoC	DPVD
Dense to very dense	VDNNV	VDNL	VDNM	VDND	VDNoC

* Refer section- Abbreviations or Table 11 and Table 13 for explanation.

a. Sampling

Many researchers have been successfully used single band, ratio indices and coefficients for detection and delineation (Chen *et al.*, 2012) of objects like forests, water bodies, barren lands, rocky lands, snow covers, marsh lands, desert lands, etc. The variations in land phenomenon regulate surface radiance according to their reflectivity (Carlson *et al.*, 1990; Chen *et al.*, 2012). Surface reflectance values are sensitive to variations in vegetation cover, soil, background temperature, thermal inertia, and topography (Bhagat 2012). Goetz (1997) has used inverse relationship between SVI and Ts based on inversion soil-vegetation-atmosphere-transfer (SVAT) model for estimating soil surface moisture using NDVI-Ts triangle space. This approach is defined as the 'Triangle Method' includes vegetation indices, soil moisture indices and thermal indices (Weng *et al.*, 2009; Lu *et al.*, 2011). Objects detected using this approach are stood more precise than single bands. Surface temperature can be estimated using thermal band and vegetation can be detected with the help of near infrared band (Nemani and Running, 1989; Carlosan *et al.*, 1990; Nemani *et al.*, 1993; Tanriverdi, 2010). Thus, all surface elements have equal importance in estimations of objects (Owen *et al.*, 1998).

Water body absorbs maximum amount of radiation and emits very little energy (Nemani *et al.*, 1993). Forest cover reflects maximum amount of Green and Near Infrared (NIR) bands and a good absorber of Blue and Red band. Chemical component existing in tree leaves known as 'chlorophyll' effectively absorbs radiation from the Blue and Red band (Jiany *et al.*, 2008). The inner structure of these leaves response as good emission of NIR wavelength (Roberts *et al.*, 2011). On the other hand, visible and NIR radiation absorb more in the form of longer wavelength from water body and less from shorter wavelength (Lu *et al.*, 2011). Thus, water appears blue-green or blue due to maximum reflectance of shorter wavelength and viewed dark because reflectance of red and near infrared depending on the suspended sediments amount in water (Fletcher and Everitt, 2007). Rocky lands are purely dry and rarely covered by thin grass and algae in wet seasons. However, rocky lands absorb very low amount of visible as well as NIR waves and reflect maximum as compare to other classes (Majed *et al.*, 2011). Water bodies, deep forests and rocky lands are stable objects and have extreme reflectance (minimum and maximum) in the region.

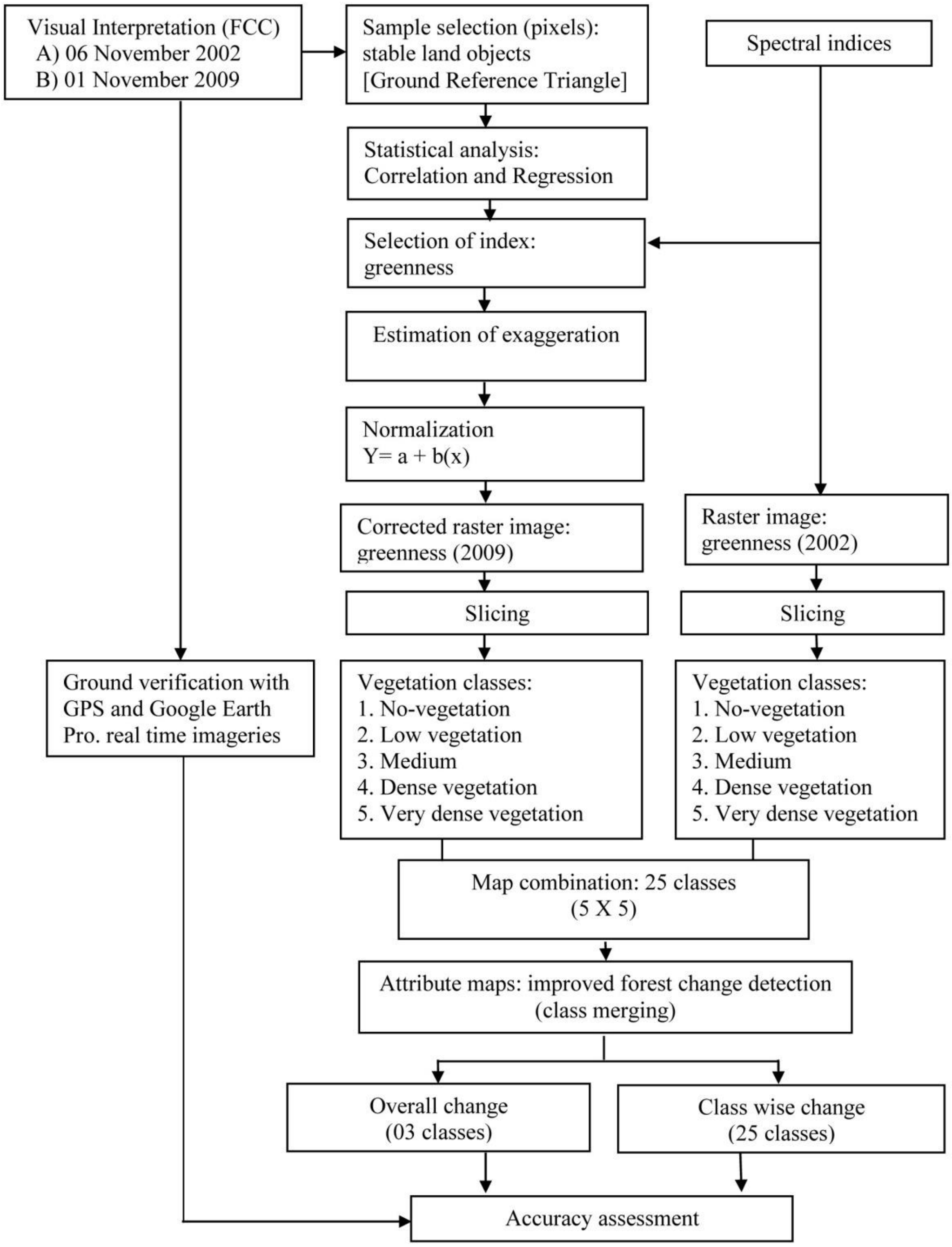

Figure 6. Approach-II: schematic preparation

The variations in reflectance recorded is satellite image have influence on accuracy of forest CD using post-classification (Pu *et al.*, 2008). Therefore, corrective approach was adopted for detection of FCD (discussed in next section). Ground truth information (170 samples) was collected for these stable land objects which were appeared and identified on satellite images e.g. Landsat-7 ETM+ (2002) and Landsat-5 TM (2009). DN values of these land objects were used further statistical analysis and normalization of indices calculated using satellite data (t_2) (Bhagat, 2012). About 31.18% samples were collected from forest cover, 27.65% from rocky land, 29.41% from water body and 11.76% from barren land for further process (Figure 7).

b. Statistical analysis

NDVI has been widely used for vegetation analysis, however, greenness (equation 5 and 6) (Crist *et al.*, 1986; Huang *et al.*, 2002) have more potential of vegetation analysis. Greenness values estimated for both images (t_1 and t_2) have positively correlated with NDVI. Therefore, greenness estimated for ETM+ (t_1) and TM (t_2) data was used as dependent variable for estimations corrected greenness values for t2 (Figure 8).

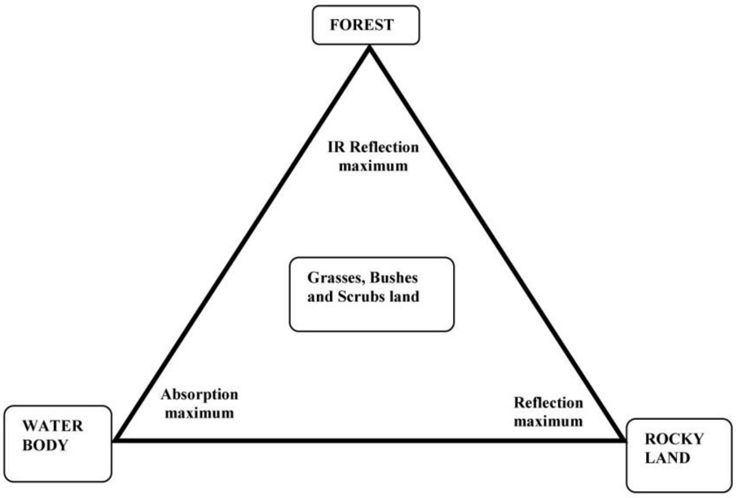

Figure 7. Ground Reference Triangle

Greenness (ETM+) =

((Band1 * (-0.3344)) + (Band2 * (-0.3544)) + (Band3 * (-0.4556)) + (Band4 * (0.6966)) + (Band5 *(-0.0242)) + (Band7* (-0.2630)) (5)

Greenness (TM) =

((Band1*(-0.2728)) + (Band2*(-0.2174))+ (Band3 * (-0.5508)) + (Band4 * (0.7221)) + (Band5 *(0.0733)) + (Band7 * (-0.1648)) (6)

NDVI (2002) values show positive correlation with greenness estimated for t_2 (2009) (r = 0.976) and NDVI (2009) with greenness for t_2 (2009) (r = 0.975) (Table 6). Scatterplot (Figure 9) for NDVI (2002) and Greenness (2009) show clustered distribution of vegetation. Therefore, calculated greenness values used for estimations of dependent variable in regression analysis. Maximum greenness (-0.07) calculated for t_1 (2002) and 65.06 for t_2 (2009) whereas minimum (-110.16) for no-vegetation i.e. water, rocky land, shadow, etc. in t_1 (2002) and -36.57 in t_2 (2009). These are stable land surface in the study area. Theoretically, values estimated for the stable lands might be same which is not possible in certain conditions at the time of image capturing (Munyati, 2004; Yarbrough *et al.*, 2005; Gill *et al.*, 2012). Therefore, accuracy of FCD in the region shows less. Further, these estimated values have been normalized using values estimated for stable pixels in this approach. Differences between estimated greenness values for stable pixels of t_1 and t_2 have been calculated and correlation with estimated indices SWI (t_1), brightness (t_1), fifth (t_1) and DN values of band 7 (t_1), band 7 (t_2), band 5 (t_1) have been estimated to find independent variables for estimation of normalized dependent variable for t_2 e.g. greenness.

Significant correlation of calculated difference between greenness estimated for stable pixels of t_1 and t_2 was estimated with band 7 (t_1), SWI (t_1), band 5 (t_1) band 7 (t_2), brightness (t_1), difference in SWI, difference in fifth (Table 7). However, the strongest correlation was estimated for band 7 of t_1 and therefore this band was used as independent variable for estimations of pixel values of correction in t_2 using regression techniques. Samples (170) collected from stable land surface i.e. forest land, rocky land, water, barren land, etc. (Figure 7) was used for this analysis.

Table 6. Correlations between NDVI and Greenness

		Greenness (2002)	**Greenness (2009)**
NDVI (2002)	Pearson correlation	0.684**	**0.976****
	Sig. (2-tailed)	.000	.000
	N	170	170
NDVI (2009)	Pearson correlation	0.571**	**0.975****
	Sig. (2-tailed)	.000	.000
	N	170	170

**** Significance at the 0.01 level (2-tailed).**

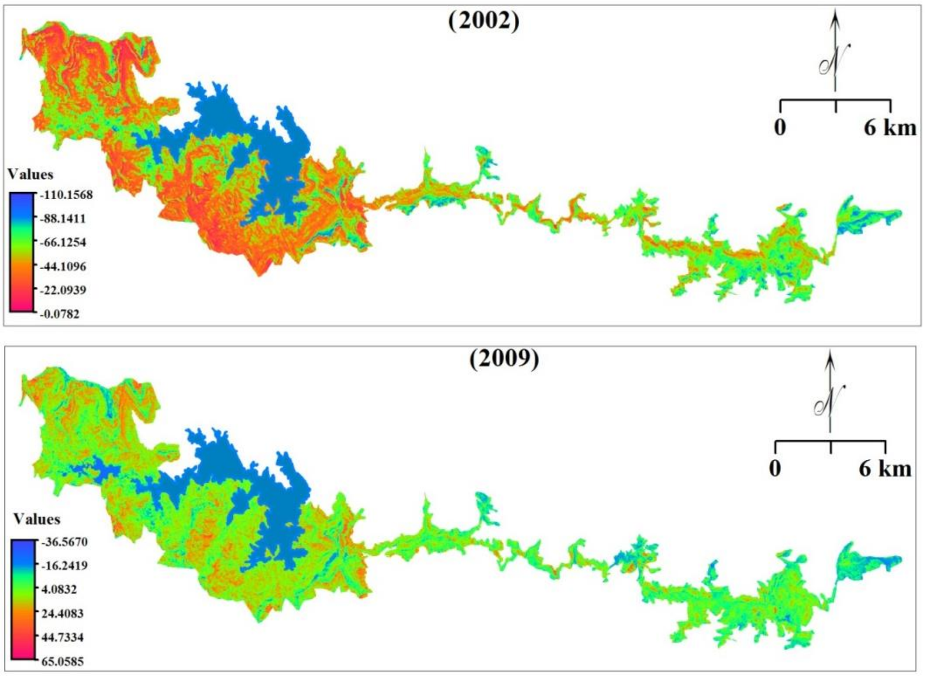

Figure 8. Greenness Index

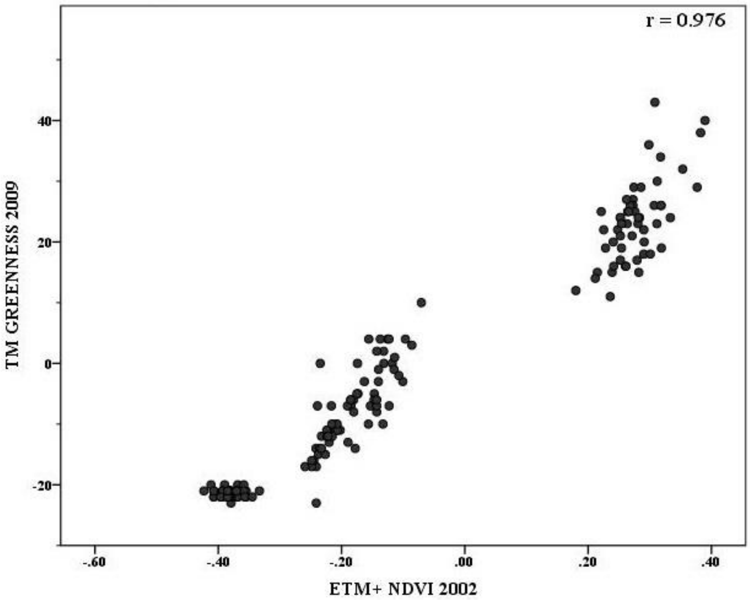

Figure 9. Scatterplot: NDVI (2002) and Greenness (2009)

Table 7. Correlation of difference greenness with selected criterion

		Band7 of t_1	SWI of t_1	Band7 of t_2	Band5 of t_1	Brightness of t_1	Difference SWI	Difference Fifth
Difference greenness	Pearson Correlation	0.983**	-0.964**	0.960**	0.960**	0.949**	0.934**	-0.933**
	Sig. (2-tailed)	0.000	0.000	0.000	0.000	0.000	0.000	0.000
	N	170	170	170	170	170	170	170

** Significance at the 0.01 level (2-tailed).

Regression (equation 7) gives mathematical tools (Lawrence and Wrlght, 2001; Cohen *et al.*, 2003) to estimate the fit between two different multi-spectral images acquired at different time for same area. Pixel values close to the regression line indicate the suitability of the model (Table 8).

$$Y = a + b(x) \tag{7}$$

Where, Y is an estimated variable (dependent), a and b are constant (a is intercept and b is rate of change in slope) and x is independent variable.

Scholars have been reported the highest change detection accuracy by using regression approach. Jiany *et al.*, (2008) reported three steps of radiometric normalization using pixel values for stable land surface: (1) delineation of stable land based on near-infrared (NIR) bands; (2) DN for stable areas using regression models, and (3) the regression coefficients used for normalizing DN of the target image. Here, linear regression model depicts (Figure 10) the fit (R^2= 0.967) of differences in Greenness of t_1 and t_2 with band 7 of t_1 with high correlation (0.983) and clustered distribution. The values closer to zero on x-axis are for water bodies, next cluster for forests and at far from the zero for barren and rocky lands. Band 5 and band 7 of ETM+ and TM images show higher sensitivity to soils and vegetation.

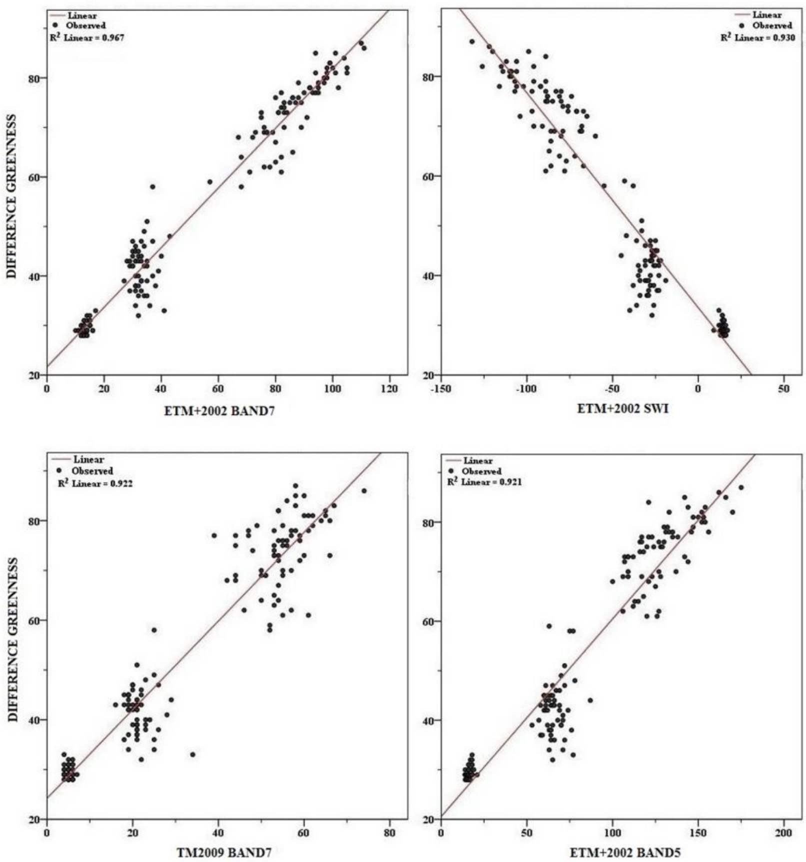

Figure 10. Regression analysis

Table 8. Regression analysis of difference greenness with selected criterion

Y	*x*	Correlation (r)	*a*	*b*	R^2	Trend
Difference greenness	Band7 of t_1	0.983	21.664	0.602	0.967	Positive
	SWI of t_1	-0.964	33.511	-0.432	0.930	Negative
	Band7 of t_2	0.96	24.208	0.891	0.922	Positive
	Band5 of t_1	0.96	20.554	0.399	0.921	Positive
	Brightness of t_1	0.949	-2.307	0.370	0.901	Positive
	Difference SWI	0.934	30.447	0.769	0.871	Positive
	Difference Fifth	-0.933	90.231	-2.110	0.871	Negative

c. Estimation of exaggeration and normalization of images

The maximum value (0.41) in reference image (t_1) (NDVI 2002) was observed for dense vegetation (Table 3) whereas minimum (-0.48) for barren land and water body with 0.05 mean and 0.16 standard deviation. Maximum NDVI value (0.71) in target image, (t_2) (2009) was observed for dense vegetation and minimum (-0.33) for no-vegetation with 0.31 mean and 0.16 standard deviation. Therefore, it is assumed that the values recorded in target image are exaggerated from ground reality (Figure 8). Regression model (equation 8) was formed to estimate the values of exaggeration in greenness (Ge) estimated for target image (t_2) for normalizing (t_2).

$$Ge = a + b\,(B7t_1) \quad (8)$$

Where, a is an intercept 21.664 and b is rate of change in slope 0.602 and $B7\,t_1$ is band 7 of reference image (t_1). Finally, raster image for greenness estimated for target image (t_2) was normalized (Nt_2) (equation 9) for final FCD.

$$Nt_2 = Greenness\ 2009 - Ge \quad (9)$$

The histograms for estimated images viz. corrected greenness 2009 using band 7 (t_1), SWI (t_1), band 7 (t_2) and band 5 (t_1), etc. were prepared in SPSS and compared with histograms prepared for greenness for t_1 and t_2 (Figure 11). Histogram values distributed from -110.1568 to -0.0782 for greenness of ETM+ (2002) and from -36.5670 to 65.0585 of TM (2009). However, distributed values on histogram prepared for corrected greenness of t_2 (2009) vary from -108.6296 to 17.5085. Similar results observed for normalized raster images of band 7 (2002), SWI (2002), band 7 (2009) and band 5 (2002).

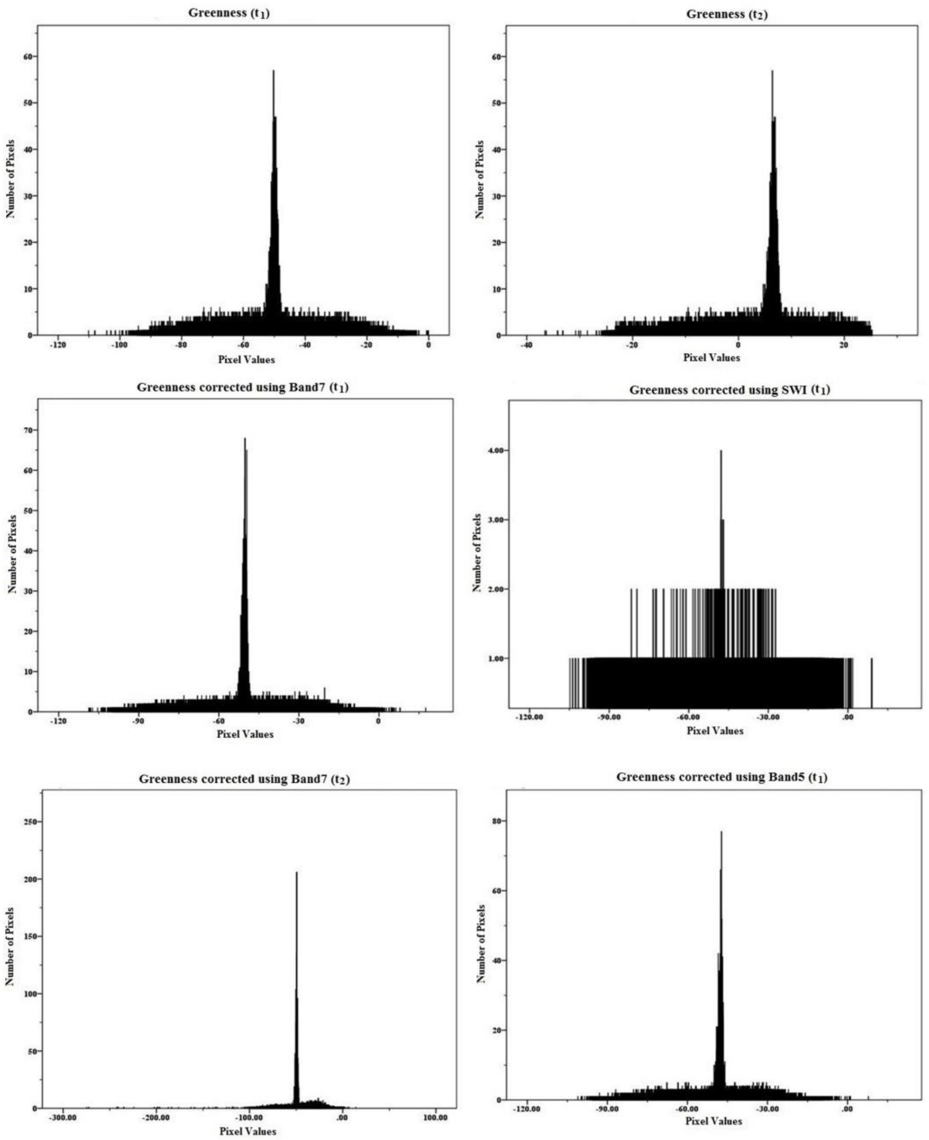

Figure 11. Histogram distributions

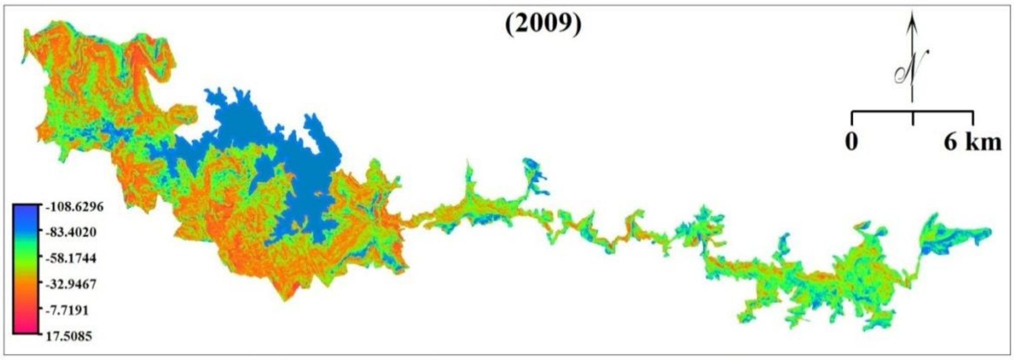

Figure 12. Corrected Greenness index

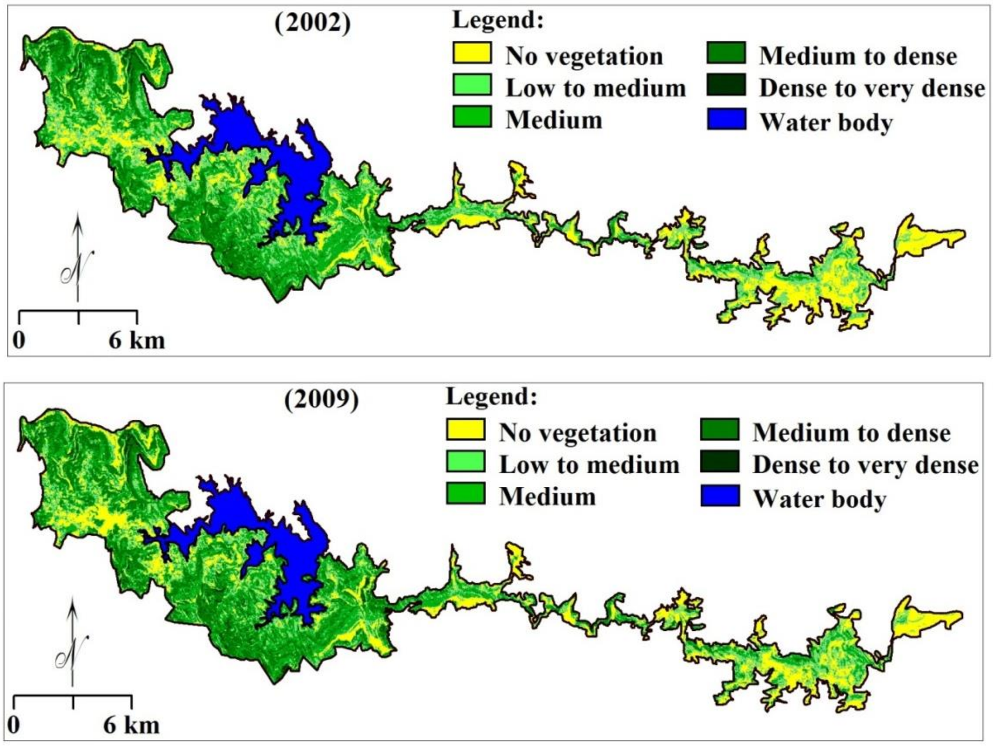

Figure 13. Distribution of forests depicted based on greenness index

4.3.3 Change detection

Finally, raster image of greenness estimated for t_1 (ETM+ 2002) and normalized raster image of greenness estimated (Figure 12) for t_2 (TM 2009) were processed for FCD in this study. The maximum value was -00.08 estimated for greenness of t_1 (2002) and 17.51 for normalized greenness (2009) whereas minimum value was -110.16 for t_1 (2002) and -108.63 for normalized image t_2 for 'no-vegetation' i.e. water, rocky land, shadow, etc. (Figure 13). Reference (t_1) and normalized (Nt_2) images were classified into five classes (Table 9) e.g. no-vegetation, low to medium, medium, medium to dense and dense to very dense, respectively.

Classified raster images (Figure 13) for 2002 and 2009 were combined using cross operation in Ilwis for forest CD. 25 classes were created in this combination and similar classes merged to get meaningful categories (Table 4). Overall changes were estimated as 'negative changes', 'positive changes' and 'no-changes'. Further, class wise changes also estimated to know the transformations from one class to another (Table 5) as 'positive change, negative change and no-change.

Table 9. Broad classification of forest density based greenness index

Vegetation classes	Index value
No-vegetation	< -64
Low to medium	-64 to -48
Medium	-48 to -32
Medium to dense	-32 to -16
Dense to very dense	-16 <

5 RESULTS

Changes in forest cover in the study area (13858.83 ha) was estimated using two approaches: Approach I) post-classification technique and Approach II) improved post-classification technique. NDVI based classified maps prepared for t_1 and t_2 were used for CD (Figure 14) in first approach and statistical analyses were performed for improvement in accuracy of post-classification CD in second approach (Figure 15). Primary field check data and pixel information of stable land units i.e. water bodies, deep forest and rocky lands were used in statistical analysis for improvement of the technique.

5.1 Approach I: Post-classification Technique

The change in forest area within period of images acquired has been detected and successfully demarcated (Figure 14). Approximately, 58.59% of reviewed area shows forests with increasing trends, 33.69% area shows no-changes and 7.72% area losing the forest. Forest cover increases for the class 'medium' vegetation about 22.41% and class 'dense to very dense' 16.84% (Table 10). Slightly negative change (-0.12%) observed for class 'no-vegetation' and the class 'medium to dense' (-2.81%) (Figure 14). Positive changes in forest cover was estimated for 8119.98 ha, no-change for 4669.29 ha and negative change for 1069.56 ha. However, these estimated values show generalized picture of changes within the classes therefore, dynamics of class wise changes also analyzed.

Sparse vegetation has been changed to medium vegetation (22.68%) and dense vegetation to very dense vegetation (15.02%) (Table 11) with no-change on 10.89 % area. However, vegetation decreases with high rate from 'low vegetation' to 'no-vegetation' for 4.30% area. The accuracy of assessment has been estimated about 77.84%, discussed in the next section (Table 14).

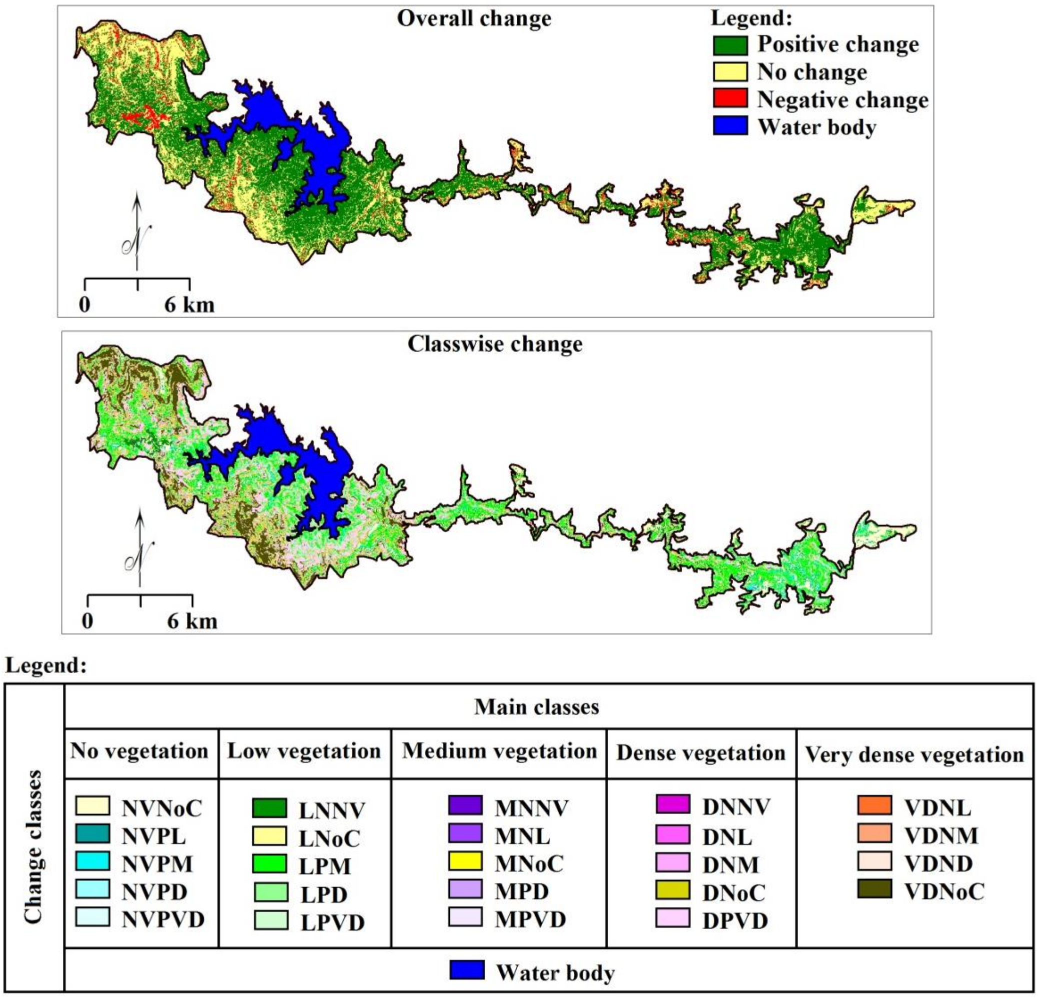

Figure 14. Approach-I: distribution of changes in forest cover

Table 10. Approach I- class wise changes in area under forest

Vegetation classes	Area (2002) ha	Area (2002) %	Area (2009) ha	Area (2009) %	Change %
No-vegetation	1713.51	12.36	1695.96	12.24	-0.12
Low to medium	5840.46	42.14	806.76	5.82	-36.32
Medium	968.4	6.99	4075.11	29.4	22.41
Medium to dense	3706.65	26.75	3317.76	23.94	-2.81
Dense to very dense	1629.81	11.76	3963.24	28.6	16.84
Total Area	**13858.8**	**100**	**13858.8**	**100**	

Table 11. Approach I – change **c**lass wise distribution of forest

Class Code	Change classes of forest	Area in ha	Area in %
NVNoC	No-vegetation to no-change	1083.96	7.8214
NVPL	No-vegetation positively changed to low vegetation	259.92	1.8755
NVPM	No-vegetation positively changed to medium vegetation	347.31	2.5061
NVPD	No-vegetation positively changed to dense vegetation	21.24	0.1533
NVPVD	No-vegetation positive changed to very dense vegetation	1.08	0.0078
LNNV	Low vegetation negatively changed to no-vegetation	597.24	4.3095
LNoC	Low vegetation with no-change	531.09	3.8321
LPM	Low vegetation positively changed to medium vegetation	3143.34	22.6811
LPD	Low vegetation positively changed to dense vegetation	1393.38	10.0541
LPVD	Low vegetation positive changed to very dense vegetation	175.41	1.2657
MNNV	Medium vegetation negative changed to no-vegetation	9.54	0.0688
MNL	Medium vegetation negatively changed to low vegetation	8.19	0.0591
MNoC	Medium vegetation with no-change	253.98	1.8326
MPD	Medium vegetation positively changed to dense vegetation	500.94	3.6146
MPVD	Medium vegetation positively changed to very dense vegetation	195.75	1.4125
DNNV	Dense vegetation negatively changed to no-vegetation	5.22	0.0377
DNL	Dense vegetation negatively changed to low vegetation	7.47	0.0539
DNM	Dense vegetation negatively changed to medium vegetation	321.48	2.3197
DNoC	Dense vegetation with no-change	1290.87	9.3144
DPVD	Dense vegetation positively changed to very dense vegetation	2081.61	15.0201
VDNNV	Very dense vegetation negatively changed to no-vegetation	0.02	0.0002
VDNL	Very dense vegetation negatively changed to low vegetation	0.07	0.0004
VDNM	Very dense vegetation negatively changed to medium vegetation	9	0.0649
VDND	Very dense vegetation negatively changed to dense vegetation	111.33	0.8033
VDNoC	Very dense vegetation with no-change	1509.39	10.8912
	Total area	**13858.83**	**100**

5.2 Approach II: Improved Post-classification Technique

Statistical techniques i.e. correlation analysis and regression model have been used to improve the performance of FCD (Figure 6). Area under forest has been detected and estimated using TCCT greenness index. However, estimated greenness has been corrected to reduce exaggeration in reflectance recorded in DN using regression model (Figure 15). About 13858.83 ha (23.59% TGA) shows positive changes, 70.8% no-change and only 6.33% area shows negative changes. Accuracy assessment shows preciseness 95.21% (Table

15) of the results compared to post-classification based FCD. 'No-changes' in vegetation observed for the class, 'low to medium' vegetation (Table 12) and positive changes for 'medium to dense' and 'dense to very dense' vegetation. This improved technique of FCD helps to reduce the exaggeration in estimations. Class wise changes also estimated to understand the dimensions of changes in forest cover (Table 13).

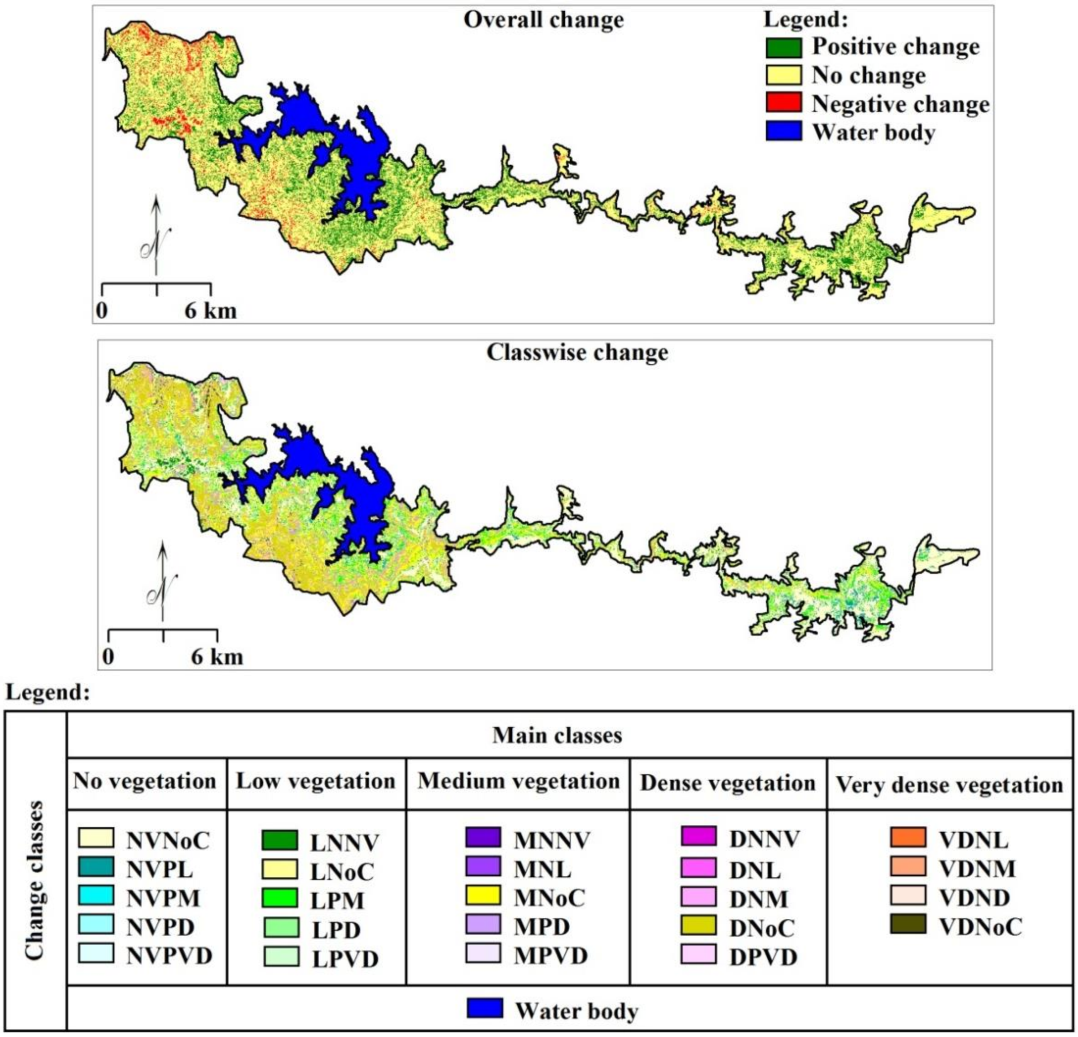

Figure 15. Approach-II: distribution of changes in forest cover

Table 12. Approach II - changes in forest cover

Vegetation classes	Area (2002) ha	%	Area (2009) ha	%	Change %
No-vegetation	3310.2	23.89	2975.22	21.47	-2.42
Low to medium	4228.47	30.51	3505.68	25.3	-5.21
Medium	4115.97	29.7	4251.24	30.68	0.98
Medium to dense	2083.95	15.04	2908.71	20.99	5.95
Dense to very dense	120.24	0.87	217.98	1.57	0.7
Total Area	**13858.83**	**100**	**13858.83**	**100**	

Table 13. Approach II – change class wise distribution of forest

Class code	Change classes of forest	Area in ha	Area in %
NVNoC	No-vegetation to no-change	1931.31	13.94
NVPL	No-vegetation positively changed to low vegetation	1176.48	8.49
NVPM	No-vegetation positively changed to medium vegetation	196.02	1.41
NVPD	No-vegetation positively changed to dense vegetation	6.3	0.05
NVPVD	No-vegetation positive changed to very dense vegetation	0.09	0.01
LNNV	Low vegetation negative change to no-vegetation	338.67	2.44
LNoC	Low vegetation negatively changed to no-vegetation	1838.99	13.27
LPM	Low vegetation with no-change	1919.72	13.85
LPD	Low vegetation positively changed to medium vegetation	168.75	1.22
LPVD	Low vegetation positively changed to dense vegetation	2.34	0.02
MNNV	Medium vegetation negative changed to no-vegetation	8.73	0.06
MNL	Medium vegetation negatively changed to low vegetation	317.43	2.29
MNoC	Medium vegetation with no-change	2262.79	16.33
MPD	Medium vegetation positively changed to dense vegetation	1511.28	10.9
MPVD	Medium vegetation positively changed to very dense vegetation	27.73	0.2
DNNV	Dense vegetation negatively changed to no-vegetation	0.34	0.01
DNL	Dense vegetation negatively changed to low vegetation	16.54	0.12
DNM	Dense vegetation negatively changed to medium vegetation	401.13	2.89
DNoC	Dense vegetation with no-change	1466.17	10.58
DPVD	Dense vegetation positively changed to very dense vegetation	98.73	0.71
VDNNV	Very dense vegetation negatively changed to no vegetation	0.17	0.01
VDNL	Very dense vegetation negatively changed to low vegetation	6.94	0.05
VDNM	Very dense vegetation negatively changed to medium vegetation	73.92	0.53
VDND	Very dense vegetation negatively changed to dense vegetation	31	0.22
VDNoC	Very dense vegetation with no-change	57.26	0.41
	Total area	**13858.83**	**100**

6 ACCURACY ASSESSMENT

Accuracy of detected changes in forest cover was estimated as user's accuracy, producer's accuracy and overall accuracy. Rahman and Saha (2008) have suggested that the sample size should take minimum 30 for each class to estimate accuracy at 90%. Therefore, 170 samples well distributed within the classes were collected using GPS points and Google Earth Pro high resolution images.

Overall accuracy of the FCD using approach I: post-classification technique was estimated about 77.84% (Table 14). User's accuracy was estimated about 58% for positively changed forest cover, 70% for no-changed or stable and 80% for negatively changed forest and 96% for water bodies. Producer's accuracy was estimated about 70% for positive changes, 78% for no-changes, 76% for negative changes and 83% for water bodies. Maximum accuracy was estimated for water bodies and negative changes in vegetation whereas positively changed vegetated area and stable land units show very less accuracy. Accuracy assessment suggests need of improvement in FCD techniques. Therefore, algorithm for improved FCD has been formulated in this study. Approach II has improved accuracy of FCD to 95.21% (Table 15) with user's accuracy about 97% for positive changes, 95% for no-change, 93% for negative changes and 96% for water bodies. Producer's accuracy was estimated about 91% for positive changes, 98% for no-change, 95% for negative changes and 96% water bodies. Thus, improved post-classification technique improves the accuracy of FCD.

Table 14. Approach-I: error matrix

Classified data	Reference data: Positive change	No-change	Negative change	Water	Row total	User's accuracy in (%)
Positive change	**19**	6	4	4	33	**58**
No-change	5	**31**	5	3	44	**70**
Negative change	2	3	**32**	3	40	**80**
Water	1	0	1	**48**	50	**96**
Column total	27	40	42	58	**167**	
Producer's accuracy (%)	**70**	**78**	**76**	**83**		
Over accuracy	**77.84**					

Table 15. Approach-II: error matrix

Classified data	Reference data: Positive change	No-change	Negative change	Water	Row total	User's accuracy (%)
Positive change	**32**	0	0	1	33	**97**
No-change	1	**42**	1	0	44	**95**
Negative change	1	1	**37**	1	40	**93**
Water	1	0	1	**48**	50	**96**
Column total	35	43	39	50	**167**	
Producer's accuracy in (%)	**91**	**98**	**95**	**96**		
Over accuracy	**95.21%**					

7 CONCLUSION

About 58.59% of reviewed area estimated using first approach of CD shows (Figure 15) positive changes, 33.69% no-change and 7.72% negative changes in forest cover in the area. However, improved post-classification analysis estimates (Table 16) about 23.59% area with positive changes, 70.08% no-change and 6.33% negative changes. Thus, normalized raster greenness image using statistical analysis removes exaggeration of reflectance recorded in satellite data and useful to estimate more precisely FCD.

Authors are aware about limitations of finer temporal resolution (7 years) and medium spatial resolution (30 x 30m) of Landsat ETM+ and Landsat TM images. The methodology and techniques formulated in this study can be useful for researchers, scholars, environmental planners and managements for change detection of forest for sustainable land management and development.

Table 16. Comparison of changes in forest cover estimated using two approaches

Change classes	Approach I: Area (hectare)	Approach I: Area (%)	Approach II: Area (hectare)	Approach II: Area (%)
Positive change	8119.98	58.59%	3269.25	23.59%
No-change	4669.29	33.69%	9712.89	70.08%
Negative change	1069.56	7.72%	876.69	6.33%
Total area	**13858.83**	**100%**	**13858.83**	**100%**

CONFLICT OF INTEREST

The authors declare no conflict of interest.

ACKNOWLEDGEMENTS

Authors gratefully acknowledge the anonymous reviewers for constructive comments and suggestions for improvement in the draft.

ABBREVIATIONS

CD: Change Detection; **DCD**: Digital Change Detection; DN: Digital Numbers, **DN**L: Dense vegetation negatively changed to low vegetation; **DNM**: Dense vegetation negatively changed to medium vegetation; **DNNV**: Dense vegetation negatively changed to no-vegetation; **DNoC**: Dense vegetation with no-change; **DPVD**: Dense vegetation positively changed to very dense vegetation; **DVI**: Difference Vegetation Index; **ERDAS**: Earth Resource Data Analysis System: **ETM+**: Enhanced Thematic Mapper Plus; **FAO**: Food and Agriculture Organization; **FCC**: False Color Composite; **FCD**: Forest Change Detection; **FSI**: Forest Survey of India; **GIS**: Geographical Information System; GPS: Global Positioning System; **ILWIS**: Integrated Land Water Information System; **IPVI**: Infrared Percentage Vegetation Index; **ISFR**: India State of Forest Report; **LAI**: Leaf Area Indices; **LNNV**: Low vegetation negatively changed to no-vegetation; **LNoC**: Low vegetation with no-change; **LPD**: Low vegetation positively changed to dense vegetation; **LPM**: Low vegetation positively changed to medium vegetation; **LPVD**: Low vegetation positive changed to very dense vegetation; **LSTI**: Land Surface Temperature Index; **MNL**: Medium vegetation negatively changed to low vegetation; **MNNV**: Medium vegetation negative changed to no-vegetation; **MNoC**: Medium vegetation with no-change; **MPD**: Medium vegetation positively changed to dense vegetation; **MPVD**: Medium vegetation positively changed to very dense vegetation; **MSAVI**: Modified **SAVI**; **MSL**: Mean Sea Level; **MSR**: Modified Simple Ratio; **NASA**: National Aeronautics and Space Administration; **NDSI**: Normalized Difference Salinity Index; **NDVI**: Normalized Difference Vegetation Index; **NIR**: Near Infrared; **NVNoC**; No-vegetation to no-change; **NVPD**: No-vegetation positively changed to dense vegetation; **NVPL**: No-vegetation positively changed to low vegetation; **NVPM**: No-vegetation positively changed to medium vegetation; **NVPVD**: No-vegetation positive changed to very dense vegetation; **RDVI**: Ratio Difference Vegetation Index; **RMS**: Route Mean Square; **RVI**: Ratio Vegetation Index; **SAVI**: Soil Adjusted Vegetation Index; **SOI**: Survey of India; SPSS: Statistical Packages for the Social Sciences; **SVAT**: Soil Vegetation Atmosphere Transfer; **SVI**: Soil Vegetation Index; **SWI**: Soil Wetness Index; **TCCT**: Tasseled Cap Coefficient Transformation; **TGA**: Total Geographical Area; **ToA**: Top of Atmosphere; **TM**: Thematic Mapper; **TVI**: Transformed Vegetation Index; **VDND**: Very dense vegetation negatively changed to dense vegetation; **VDNL**: Very dense vegetation negatively changed to low vegetation; **VDNM**: Very dense vegetation negatively changed to medium vegetation; **VDNNV**: Very dense vegetation negatively changed to no vegetation; **VDNoC**: Very dense vegetation with no-change; **WCMC**: World Conservation Monitoring Centre; **WRI**: World Resources Institute.

REFERENCES

Adegoke J. O. and Carletion A. M., 2002. Relations between soil moisture and satellite vegetation indices in the U.S. Corn Belt. *Journal of Hydrometeorology*, 3, 395-405.

Bauer M. E., Burk T. E., Ek A. R., Coppin P. R., Lime S. D., Walsh T. A., Walters D. K., B. William and Heinzen, D. F. 1994. Inventory of Minnesota forest resources with Landsat TM data. *Photogramm. Eng. Remote Sensing*, 60, 287-298.

Bhagat V. S. and Sonawane K. R., 2010. Use of LANDSAT ETM+ Data for delineation of water bodies in hilly zones. *Journal of Hydroinformatics*, 13, 661-671, http://dx.doi.org/10.2166/hydro.2010.018

Bhagat V. S., 2012. Use of Remote Sensing Techniques for Robust Digital Change Detection of Land: A Review. *Recent Patents on Space Technology*, 2 (2), 123-144.

Bhagat V.S., 2009. Use of LANDSAT ETM+ data for detection of potential areas for afforestation. *International Journal of Remote Sensing, 30, 2607-2617,* http://dx.doi.org/10.1080/01431160802552793

Breda N.J., 2003. Ground-based measurements of leaf area index: a review of methods, instruments and current controversies. *Journal of Experimental Botany*, 54, 2403-2417.

Burnicki A.C., Brown D. G. and Goovaerts P., 2010. Propagating error in land-cover-change analyses: impact of temporal dependence under increased thematic complexity. *International Journal of Geographical Information Science*, 24, 1043-1060.

Cano F., Cerrillo R. M. N., Ferrer A. G., De La Orden M.S., 2006. Detection of forest decline using IKONOS sensor for Cork Oak woods in South Spain. *Geocarto International*, 21, 13-18.

Carlowicz M., 2012. Seeing Forests for the Trees and the Carbon: Mapping the World's Forests in Three Dimensions.

Carlson T. N., Perry E. M. and Schmugge T. J. 1990. Remote estimation of soil moisture availability and fractional vegetation cover for agricultural fields. *Agriculture for Meteorology*, 52, 45-69.

Chander G. and Markham B., 2003. Revised Landsat-5 TM radiometric calibration procedures and postcalibration dynamic ranges. *IEEE Transactions on Geoscience and Remote Sensing*, 41 (11), 2674−2677.

Chandio I.A., Matori A.N., Lawal D.U., Sabri S., 2011. GIS-based land suitability analysis using AHP for public parks planning in Larkana City. *Mod. Appl. Sci*. 5 (4), 177–189.

Chapelle O., Vapnik V., Bousquet O. and Mukherjee S., 2002. Choosing multiple parameters for support vector machines. *Machine Learning*, 46, 131–159.

Chan J. C. W., Chan K. P. and Yeh A. G. O., 2001. Detecting the nature of change in an urban environment: A comparison of machine learning algorithms. *Photogrammetric Engineering & Remote Sensing*, 67 (2), 213-225.

Chen G., Hay G. J., Carvalho Luis M. T. and Wulder M. A., 2012. Object-based change detection. *Int. J. Remote Sens.*, 33, 4434-4457.

Chowdhury A. B., Paul C. J., Martyn G. F. and Geoff K. F. 2005. The role of cuticular waxes and surface roughness in determining the insecticidal efficacy of deltamethrin and dimethoate applied as emulsifiable concentrates to leaf surfaces. *International Journal of Pest Management*, 51, 253-263.

Clifton C., 2003. Change detection in overhead imagery using Neural Networks. *Applied Intelligence*, 18, 215-234.

Cohen W. B., Fiorella M., Gray J., Helmer E. and Anderson K., 1998. An efficient and accurate method for mapping forest clearcuts in the Pacific Northwest using Landsat imagery. *Photogram. Eng. Remote Sens.*, 64, 293-300.

Cohen W. B., Maierspergerb T. K., Gowerc S. T. and Turner D. P., 2003. An improved strategy for regression of biophysical variables and Landsat ETM+ data. *Remote Sens. Environ*., 84, 561-571.

Coppin P. and Bauer M., 1996. Digital change detection in forest ecosystems with remote sensing imagery. *Remote Sensing Reviews*, 13, 207- 234.

Coppin P., Jonckheere I., Nackaerts K., Muys B. and Lambin E., 2004. Digital change detection methods in ecosystem monitoring: a review. *Int. J. Remote Sens.*, 25, 1565-1596.

Crist E. P. and Kauth R. J., 1986. The tasseled cap de-mystified, *Photogram. Eng. Remote Sen*., 52, 81-86.

Dhakal A. S., Amada T., Aniya M. and Sharm R. R., 2002. Detection of areas associated with flood and erosion caused by a heavy rainfall using multitemporal Landsat TM data, *Photogram. Eng. Remote Sens*., 68, 233-239.

Drescher M. and Perera A. H., 2010. Comparing two sets of forest cover change knowledge used in forest landscape management planning. *Journal of Environmental Planning and Management*, 53 (5), 591-613.

Du Y., Teillet P. M. and Cihlar J., 2002. Radiometric normalization of multitemporal high-resolution satellite images with quality control for land cover change detection. *Remote Sensing Environment*, 82, 123-134.

Ehlers M., Klonus S., Astrand P. J. and Rosso P., 2010. Multi-sensor image fusion for pansharpening in remote sensing. *International Journal of Image and Data Fusion*, 1, 25-45.

Fang H. and Xu J., 2000. Land cover and vegetation change in the Yellow river delta nature reserve analysed with Landsat Thematic Mapper data. *Geocarto International*, 15, 43-50.

Fastring D. R. and Griffith J. A., 2009. Malaria incidence in Nairobi, Kenya and decadal trends in NDVI and climatic variables. *Geocarto International*, 24 (3), 207-221.

Felkar P., Cannell G. H. and Clark P. R., 1981. Variation in growth among 13 Prosopis (mesquite) species. *Experimental Agriculture*, 28, 209-218.

Fettig C. J., Klepzig K. D., Billings R. F., Munson A. S., Nowak J. T., Nebeker T. E., and Negro J. F., 2007. The effectiveness of vegetation management practices for prevention and control of bark beetle infestations in coniferous forests of the western and southern United States, *Forest Ecology and Management*, 238, 24-53.

Fletcher R. S. and Everitt J. H., 2007. A six-camera digital video imaging system sensitive to visible, red edge, near-infrared, and mid-infrared wavelengths. *Geocarto International*, 22 (2), 75-86.

Food and Agriculture Organisation (FAO), 2015. Global Forest Resources Assessment 2015. Available online at http://www.fao.org/3/a-i4793e.pdf

Forkuo E. K. and Frimpong A., 2012. Analysis of Forest Cover Change Detection. *International Journal of Remote Sensing Applications*, 2 (4), 82-92.

Gareeau R. M., Gutierrez M., Ham T., Nemethy J. and Hackett J., 2009. Geospatial image change detecting system and associated method. US 7528938 B2.

Ghosh A., Mishra N. S. and Ghosh S., 2011. Fuzzy clustering algorithms for unsupervised change detection in remote sensing images. *Information Sci.*, 181 (4), 699–715

Gill T.K., Danaher T., Gillingham S.S. and Mitchell R.M., 2012. Comparing bright- target surface spectral-reflectance estimates obtained from IRS P6 LISS III to those obtained from Landsat 5 TM and Landsat 7 ETM+. *Remote Sensing Letters*, 3 (2), 121-130.

Giri Babu D., Raja Shekhar S. S., Chandrasekar K., Sesha Sai M. V. R., Diwakar P. G. and Dadhwal V.K., 2014. Automatic image registration using free and open source software. *The International Archives of the Photogrammetry, Remote Sensing and Spatial Information Sciences*, XL-8, 1121-1128.

Globle Climate Observaion System (GCOS), 2010. Implementation plan for the Global Observing System for Climate in support of the UNFCCC. GCOS-138, WMO-TD/No. 1523, 1-136.

Goetz S. J., 1997. Multi-sensor analysis of NDVI, surface temperature and biophysical variables at a mixed grassland site. *Int. J. Remote Sens*., 18, 71-94.

Golmehr E., 2008. A remote sensing evaluation for agronomic land use mapping in Tehran Province, *Iran. J. Appl. Sci. Environ.* Manage., 12 (2), 43-46.

Hansen H. O., 2000. An AIDS model with reproduction with an application based on data from Uganda. *Mathematical Population Studies*, 8, 175-203.

Hara G. C., Cheriyadat A., Seo S. and Vijayaraj V., 2012. Change Analyst, US 8160296 B2.

Hayes D. and Sader S. A., 2001. Change detection techniques for monitoring forest clearing and regrowth in a tropical moist forest. *Photogrammetric Engineering and Remote Sensing*, 67, 1067-1075.

Healey S. P., Cohen W. B., Zhiqiang Y. and Krankina O. N., 2008. Comparison of tasseled cap-based Landsat data structures for use in forest disturbance detection. *Remote Sens. Environ.*, 97, 301-310.

Huang C., Wylie B., Yang L., Homar C. and Zylstra G., 2002. Derivation of a tasselled cap transformation based on Landsat-7 at-satellite reflectance. *International Journal of Remote Sensing*, 23, 1741-1748.

Huete A., Didan K., Miura T., Rodriguez E. P., Gao X. and Ferreira L. G., 2002. Overview of the radiometric and biophysical performance of the MODIS vegetation indices. *Remote Sens. Environ.*, 83, 195-213.

Im J., Jensen J. R. and Tullis J. A., 2008. Object-based change detection using correlation image analysis and image segmentation. *International Journal of Remote Sensing*, 29 (2), 399-423.

Jensen R. R., 2002. Spatial and temporal leaf area index dynamics in a North Central Florida, USA Preserve. *Geocarto International*, 17 (4), 47-54.

Jiany G., Haiganga S., Guoruia M. and Qiming Z., 2008. A review of multi-temporal remote sensing data change algorithms, The International Archives of the Photogrammetry. *Remote Sens. Spatial Infor. Sci.*, 37 (B7), 757-762.

Jonckheere I., Fleck S., Nackaerts K., Muysa B., Coppin P., Weiss M. and Baret F., 2004. Review of methods for in situ leaf area index determination Part I. Theories, sensors and hemispherical photography. *Agricultural and Forest Meteorology*, 121, 19-35.

Julien Y., Sobrino J. A., Mattar C., Ruescas B., Jimenez-mun J. A., Sorai G., Hidalgo V., Atitar M., Franch B. and Cuenca J., 2011. Temporal analysis of normalized difference vegetation index (NDVI) and land surface temperature (LST) parameters to detect changes in the Iberian land cover between 1981 and 2001. *International Journal of Remote Sensing*, 32, 2057-2068.

Keenan R. J., Lamb D., Parrotta J. and Kikkawa J., 1999. Ecosystem management in tropical timber plantations. *Journal of Sustainable Forestry*, 9 (1-2), 117-134.

Kennedy R. E., Townsend P. A., Gross J. E., Cohen W. B., Bolstad P., Wang Y. Q. and Adams P., 2009. Remote sensing change detection tools for natural resource managers: Understanding concepts and tradeoffs in the design of landscape monitoring projects. *Remote Sens. Environ*., 113, 1382-1396.

Kim A. M., Lui D. and Gong P., 2004. Change detection from SOPT Panchromatic imagery at the urban-rural fringe of Ho Chi Minh City, Vietnam. *Geographic Information Sci.*, 10, 42-48.

Kumsap C., Borne F. and Moss D., 2005. The technique of distance decayed visibility for forest landscape visualization. *International Journal of Geographical Information Science*, 19 (6), 723-744.

Lawrence R. and Wrlght A., 2001. Rule-based classification systems using classification and regression tree (CART) Analysis. *Photogram. Eng. Remote Sens.*, 67, 1137-1142.

Lippitt C. D., Coulter L. L., Freeman M., Lamantia J., Pang W. and Stow D. A., 2011. The effect of input data transformations on object based image analysis. *Remote Sensing Letters*, 3, 21-29.

Lu D., Moran E. and Hetrick S., 2011. Detection of impervious surface change with multitemporal Landsat images in an urban-rural frontier. *ISPRS J. Photogrammetry Remote Sens.*, 66, 298-306.

Lunetta R. S., Knight J. F., Ediriwickrema J., Lyon J. G. and Worthy L. D., 2006. Land-cover change detection using multi-temporal MODIS NDVI data. *Remote Sens. Environ.*, 105, 142- 154.

Majed M. A. Z., Abdullah T. and Abdulrahman A. A., 2011. Soil erosion control and moisture conservation of arid lands with stone cover. *Arid Land Research and Management*, 25 (3), 294-307.

Mishra A., Sharma S. D. and Gupta M. K., 2003. Soil rehabilitation through afforestation: Evaluation of the performance of Prosopis juliflora, Dalbergia sissoo, and Eucalyptus tereticornis plantations in a sodic environment, *Arid Land Research and Management*, 17, 257–269.

Morisette J. T., Baret F., Privette J. L., Myneni R. B., Nickeson J. E., Garrigues S., Shabanov N. V., Weiss M., Fernandes R. A., Leblanc S. G., Kalacska M., Sánchez-Azofeifa G. A., Chubey M., Rivard B., Stenberg P., Rautiainen M., Voipio P., Manninen T., Pilant A. N., Lewis T. E., Iiames J. S., Colombo R., Meroni M., Busetto L., Cohen W.B., Turner D. P., Warner E. D., Petersen G. W., Seufert G., and Cook R., 2006. Validation of global moderate-resolution LAI products: A framework proposed within the CEOS land product validation subgroup. *IEEE Transactions on Geoscience and Remote Sensing*, 44, 1804-1817.

Mountrakis G., Im J. and Ogole C., 2011. Support vector machines in remote sensing: A review. *ISPRS Journal of Photogrammetry Remote Sensing*, 66(3), 247–259.

Mróz M. and Sobieraj A., 2004. Comparison of several vegetation indices calculated on the basis of a seasonal SPOT XS time series, and their stability for land cover and agricultural crop identification. *Technical Sciences*, 7, 40-66.

Munyati C., 2004. Use of principal component analysis (PCA) of remote sensing images in wetland change detection on the Kafue Flats, Zambia. *Geocarto Int.*, 19, 11-22.

NASA. *Landsat 7 Science Data Users Handbook*.

Nemani R. R. and Running S. W., 1989. Estimation of regional surface resistance to evapotranspiration from NDVI and Thermal-IR AVHRR data. *J. Appl. Meteorol*, 28, 276-284.

Nemani R., Pierce L., Running S. W. and Goward S., 1993. Developing satellite derived estimates of surface moisture status. *J. Appl. Meteorol*, 32, 548-557.

Owen T. W., Carlson T. N. and Gillies R. R., 1998. An assessment of satellite remotely-sensed land cover parameters in quantitatively describing the climatic effect of urbanization. *International Journal of Remote Sensing*, 19, 1663 -1681.

Pajares G., Alonso C., Cruz J. M. and Moreno V., 2002. Shade identification in urban areas through the bayesian classifier, *Proc. European Symposium on Intelligent Technologies*, 476-481.

Panigrahy S., Anitha D., Kimothi M. M. and Singh S. P., 2010. Timberline change detection using topographic map and satellite imagery. Tropical Ecology, 51, 87-91.

Pant T., Singh D. and Srivastava T., 2010. The potential application of fractal approach for surface roughness retrieval: A study for simulated surfaces. *Geomatics Natural Hazards and Risk*, 1, 243-257.

Petit C. C. and Lambin E. F., 2001. Integration of multi-source remote sensing data for land cover change detection. *International Journal of Geographical Information Science*, 15, 785-803.

Pouliot D. A., King D. J, Bell F. W. and Pitt D. G., 2002. Automated tree crown detection and delineation in high-resolution digital camera imagery of coniferous forest regeneration. *Remote Sens. Environ*., 82, 322-334.

Pu R., Gong P., Tian Y., Miao X., CarruthersI R. I. and Anderson G. L., 2008. Invasive species change detection using artificial neural networks and CASI hyperspectral imagery. Environ Monitoring Assessment, 140, 5-32.

Rahman R. and Saha S. K., 2008. Multi-resolution segmentation for object-based classification and accuracy assessment of land Use /land cover classification using remotely sensed data. *Journal of the Indian Society of Remote Sensing*, 36, 189-201.

Roberts J. W., Aardt J. A. N. V. and Ahmed F. B., 2011. Image fusion for enhanced forest structural assessment. *International Journal of Remote Sensing*, 32 (1), 243-266.

Rozenstein O. and Karnieli A., 2011. Comparison of methods for landuse classification incorporating remote sensing and GIS inputs. *Applied Geography*, 31, 533-544.

Schwilch G., Bestelmeyer B., Bunning S., Critchley W., Herrich J., Kellner K., Liniger H. P., Nachtergaele F., Ritsema C. J., Schuster B., Tabo R., Lynden G. V. and Winslow M., 2011. Experiences in monitoring and assessment of sustainable land management. *Land Degrad. Develop.*, 22, 214-225.

Shalaby A., Ouma Y. O. and Tateishi R., 2006. Land suitability assessment for perennial crops using remote sensing and geographic information systems: a case study in North-Western Egypt. *Arch. Agron. Soil Sci*., 52 (3), 243–261.

Silleos N. G., Alexandridis T. K., Gitas I. Z. and Perakis K., 2006. Vegetation indices: advances made in biomass estimation and vegetation monitoring in the last 30 years. *Geocarto International*, 21 (4), 21-28.

Singh A., 1989. Digital change detection techniques using remotelysensed data. *Internation Journal of Remote Sensing*, 10, 989-1003.

Singh G., 1996. Effect of site preparation techniques on Prosopis juliflora in an alkali soil. *Forest Ecology and Management*, 80, 267-278.

Sommer S., Zucca C., Grainger A., Cherlet M., Zougmore R., Sokona Y., Hill J., Della R., Peruta J. R. and Wang G., 2011. Application of indicator systems for monitoring and assessment of desertification from national to global scales, *Land Degradation Development*, 22, 184-197.

Southworth J., Munroe D. and Nagendra H., 2004. Land cover change and landscape fragmentation-comparing the utility of continuous and discrete analyses for a Western Honduras region. *Agriculture Ecosystems and Environment*, 101, 185-205.

Tanriverdi C., 2010. Improved agricultural management using remote sensing to estimate water stress indices. *Application in Remote Sensing Journal*, 1, 19-24.

Theiler J. P. and Perkins J. S., 2011. Anomalous change detection in imagery, US 7953280 B2.

Tsai F. and Lin H. C., 2007. Polygon-based texture mapping for cyber city 3D building models. *International Journal of Geographical Information Science*, 21 (9), 965-981.

Turker M. and Derenyi E., 2000. GIS assisted change detection using remote sensing. *Geocarto Int.*, 15 (1), 51-56.

Virk R. and King D., 2006. Comparison of techniques for forest change mapping using Landsat data in Karnataka, *India*. *Geocarto Int*., 21, 49-57.

Weng Q., 2009. Thermal infrared remote sensing for urban climate and environmental studies: Methods, applications and trends. *ISPRS J. Photogrammetry Remote Sens.*, 64, 335-344.

Yang G. G., Qu S. L., Jian H. F., Bao Y. H., Hong B. F., and Ze J. T., 2014. Identification of heavy metal sources in the reclaimed farmland soils of the pearl river estuary in China using a multivariate geostatistical approach. *Ecotoxicology and Environmental Safety*, 105, 7-12.

Yarbrough L. D., Easson G. and Kuszmaul J. S., 2005. Using at-sensor radiance and reflectance tasseled cap transforms applied to change detection for the ASTER sensor. *Analysis of Multi-Temporal Remote Sensing Images*, 16, 41-145.

Yuan F. and Bauer M. E., 2007. Comparison of impervious surface area and normalized difference vegetation index as indicators of surface urban heat island effects in Landsat imagery. *Remote Sensing of Environment*, 106, 375 - 386.

Zhang Q., Wang J., Peng X., Gong P. and Shi P., 2002. Urban build-up land change detection with road density and spectral information from multitemporal Landsat TM data. *International Journal of Remote Sensing*, 23, 3057–3078.

Zolekar R. B. and Bhagat V. S., 2015. Multi-criteria land suitability analysis for agriculture in hilly zone: Remote sensing and GIS approach. *Computers and Electronics in Agriculture*, 118, 300-321.

******